

Anytime-Valid Federated Conformal RAG for LLM Swarms

Prasanjit Dubey  Xiaoming Huo 

H. Milton Stewart School of Industrial and Systems Engineering,
Georgia Institute of Technology, Atlanta, GA 30332, U.S.A.

Abstract

Federated Conformal RAG (FC-RAG) [Dubey and Huo, 2026] provides distribution-free coverage for a bandwidth-limited swarm of weak language models, but only at a fixed horizon. We extend it to anytime-valid sequential coverage: validity at every stopping time, preserved under predictable adaptive control (recalibration, per-node bandwidth escalation, distilled-student refresh), at no extra cost in assumptions over fixed-horizon FC-RAG. Naive composition of fixed-horizon FC-RAG with off-the-shelf sequential testing fails because FC-RAG’s marginal coverage bound makes the natural betting e -process a non-supermartingale on adverse calibration draws, and Ville’s inequality cannot be invoked. We give *Anytime-FC-RAG*, a sequential extension built on a *summable per-step calibration-deviation budget* that converts the marginal bound into a strict conditional bound on a calibration-good event, paired with a *truncated betting e -process* that is a nonnegative supermartingale on the entire probability space. From these two ingredients, we obtain four guarantees: time-uniform alarm validity $\mathbb{P}(\sup_t E_t \geq 1/\delta_e) \leq \delta_e + \delta_{\text{cal}}$, a Hoeffding-stitched cumulative-miscoverage envelope at the same total budget, safety under any predictable controller (recalibration, bandwidth escalation, student refresh), and training-side error propagation across an unbounded sequence of Federated Probe-Logit Distillation (FPLD) refreshes via a summable training budget. As a practical consequence, an adaptive controller that escalates retrieval bandwidth only when the e -process crosses a warning threshold matches the alarm rate of a fixed-high-bandwidth schedule at substantially lower communication cost. Synthetic and end-to-end experiments on a GPT-2-small + MiniLM swarm across MMLU, DBpedia, and AG News verify the predicted alarm rate, detection delay, envelope coverage, and 14–57% bandwidth savings; the alarm fires when and only when coverage genuinely breaks, not on every drift.

1 Introduction

Federated Conformal RAG (FC-RAG) [Dubey and Huo, 2026] provides a distribution-free coverage guarantee for the answer set produced by a bandwidth-limited swarm of weak language models, but only at a fixed horizon. Real deployments are sequential: operators inspect coverage across the answered-query stream, recalibrate when the rolling buffer freshens, and may escalate per-node retrieval bandwidth or refresh a distilled student in response to observed drift. The fixed-horizon guarantee does not apply once any of these actions is taken. This paper asks how to deliver time-uniform coverage and safe

adaptive control on top of FC-RAG without strengthening the i.i.d.-deployment-data assumption that fixed-horizon FC-RAG already relies on, and how to propagate the underlying federated training rate across an unbounded sequence of student refreshes while preserving the sequential guarantee.

As a running example throughout this paper, consider the $K = 4$ topic-specialized GPT-2-small + MiniLM retrieval swarm of [Dubey and Huo, 2026, §7.5]: four nodes serving MMLU subjects `high_school_statistics`, `high_school_physics`, `high_school_biology`, and `high_school_world_history`, each retrieving from its own subject-specific corpus and uploading bandwidth-limited score summaries to a hub that emits a conformal answer set at level $1 - \alpha = 0.9$. A reasonable operational goal is to monitor coverage across the answered-query stream and, if the corpus on `high_school_biology` drifts after an update, fire an alarm and selectively escalate that node’s bandwidth without forfeiting the statistical guarantee already accumulated on the other three subjects.

This operational goal is harder than a naive composition of fixed-horizon FC-RAG and off-the-shelf sequential testing would suggest. The natural betting e-process built on FC-RAG’s marginal coverage bound fails the supermartingale property on adverse calibration draws, so Ville’s inequality cannot be applied off-the-shelf. Adaptive controller actions further change the test centering mid-stream in a way that compounds the difficulty, and the underlying student model may be refreshed multiple times during deployment, so training-side error must propagate cleanly across an unbounded sequence of refreshes. The construction we introduce closes all three gaps via a summable per-step calibration-deviation budget paired with a truncated supermartingale, and the resulting guarantees apply to any sequential conformal protocol with a predictable slack decomposition, beyond the RAG instance considered here (Section 6).

Limitations of prior work. Three lines of work each cover a piece of this question but leave a gap.

- **Fixed-horizon FC-RAG.** The base FC-RAG protocol [Dubey and Huo, 2026] controls a one-shot marginal coverage guarantee; sequential monitoring with optional stopping or adaptive intervention breaks the guarantee.
- **Single-site conformal RAG.** TRAQ [Li et al., 2024] and conformal-RAG-style work [Chakraborty et al., 2026] apply split-conformal to RAG QA pipelines but assume one model, one corpus, and one calibration set, with no federation, no bandwidth charging, and no sequential validity.
- **Conformal test martingales.** Conformal test martingales [Vovk et al., 2021] give a time-uniform changepoint-detection construction over exchangeable data, but in a single-site setting with no slack decomposition (no Δ_{FL} , Δ_{RAG} , Δ_{train}) and no model for federated calibration with bandwidth budgets.

Centralized sequential testing tools [Ramdas et al., 2023, Howard et al., 2020, 2021, Waudby-Smith and Ramdas, 2024, Gauthier et al., 2025, Hultberg et al., 2026, Gibbs and Candes, 2021, Angelopoulos et al., 2024b] and federated conformal methods [Lu et al., 2023, Plassier et al., 2023, Wen et al., 2026, Xu et al., 2025] cover related ground but not this composition; no prior result gives a time-uniform reliability guarantee for a federated LLM swarm whose retrieval and calibration messages are simultaneously communication-constrained. Table 1 summarizes the joint capability gap.

Table 1: Capabilities of related approaches. The combination of time-uniform validity, a bandwidth-charged slack decomposition, federated calibration with summary compression, training-side propagation, and validity under predictable controller actions is jointly absent from prior work.

| Approach | Time-uniform | Bandwidth-charged slack | Federated calibration | Training propagation | Predictable controller |
|----------------------------------------------------------------------------------------------------|--------------|-------------------------|-----------------------|----------------------|------------------------|
| FC-RAG [Dubey and Huo, 2026] | × | ✓ | ✓ | ✓ | × |
| Conformal test martingales [Vovk et al., 2021] | ✓ | × | × | × | × |
| Online conformal [Gibbs and Candes, 2021, Angelopoulos et al., 2024b] | ✓* | × | × | × | — |
| Federated conformal [Lu et al., 2023, Plassier et al., 2023, Wen et al., 2026, Xu et al., 2025] | × | partial | ✓ | × | × |
| Anytime-FC-RAG (ours) | ✓ | ✓ | ✓ | ✓ | ✓ |

* Long-run average coverage via adaptive step size; not strictly per-step time-uniform.

Constraints and goal. We adopt three operational constraints inherited from FC-RAG [Dubey and Huo, 2026]: (i) no gradient or weight exchange; (ii) no data pooling; (iii) per-uplink budgets $B_{i,t}$ (per-query inference) and B_t^{cal} (per-refresh calibration) are first-class. The goal is to characterize whether a sequential extension can admit a strict conditional bound $\mathbb{E}[M_t \mid \mathcal{F}_{t-1}] \leq b_t = \alpha + 1/(n_{\text{cal},t} + 1) + \Delta_{\text{FL},t} + \Delta_{\text{RAG},t} + \Delta_{\text{train},t}$ on a calibration-good event G_t , with the same slack decomposition as fixed-horizon FC-RAG. We further require that this bound be preserved under any predictable controller (recalibration, bandwidth escalation, student refresh). Our aim is to characterize what is provably achievable, not to demonstrate a deployment-ready system.

Contributions.

1. **Anytime-FC-RAG protocol** (Section 3): a sequential extension of FC-RAG in which a swarm answers a stream of queries, updates compressed calibration summaries on a rolling buffer, and maintains a betting e-process for alarm-triggered intervention.
2. **Cal-deviation budget and alarm validity** (Lemmas 4.5, 4.6, Theorem 4.7): a summable per-step budget $\{\delta_t^{\text{cal}}\}$ defines an \mathcal{F}_{t-1} -measurable calibration-good event G_t on which the per-step miscoverage admits a *strict* conditional bound; the truncated betting e-process $\tilde{E}_t = E_t \mathbf{1}_{\cap_{s \leq t} G_s}$ is then a nonnegative supermartingale on the entire probability space, and Ville plus splitting on G_t gives $\mathbb{P}(\sup_t E_t \geq 1/\delta_e) \leq \delta_e + \delta_{\text{cal}}$.
3. **Cumulative-miscoverage envelope and safe adaptive control** (Theorems 4.9, 4.11): a time-uniform Hoeffding boundary $u_t(\delta)$ controls the empirical miscoverage rate against the predictable slack at probability $\geq 1 - \delta$, and any predictable controller preserves both this envelope and the alarm guarantee.
4. **Training-to-deployment propagation** (Theorem 4.12): an FTC chain inheriting the (B5') clause of base FC-RAG [Dubey and Huo, 2026, Cor. 3] gives $\Delta_{\text{train},t} \leq$

$f_{\max,t}(\bar{K}_t + \sqrt{2\bar{K}_t})$ simultaneously over t on an event of probability $\geq 1 - \delta_{\text{train}}$, for a summable budget $\sum_r \delta_r \leq \delta_{\text{train}}$.

Scope. This work establishes a time-uniform reliability guarantee for federated LLM swarms with bandwidth-constrained retrieval and calibration, paired with end-to-end empirical validation on a $K = 4$ GPT-2-small + MiniLM swarm. Privacy accounting, delayed-label handling, adversarial-node and architecture-heterogeneous regimes, and deployment-scale benchmarking are natural extensions of the same machinery and are deferred to follow-up work.

Paper roadmap. Section 2 specifies the sequential deployment model. Section 3 states the Anytime-FC-RAG protocol. Section 4 proves the four theorems (alarm validity, envelope, safe control, training propagation). Section 5 reports synthetic, real-world, and comparative experiments validating the four theorems on a GPT-2-small + MiniLM swarm across three benchmarks. Section 6 situates the contribution against prior work and discusses limitations.

2 Problem setup

We study sequential discrete-answer prediction in a federated swarm of weak language models constrained by a bandwidth budget. This section fixes the data, communication, filtration, and estimand formalism that the planned theorems will refer to; the concrete protocol sits in Section 3.

2.1 Data, swarm, and communication

Let \mathcal{X} denote the query or context space and let \mathcal{Y} be a finite answer space (multiple-choice-style QA, label prediction, or a bounded candidate set extracted from a top- p truncation of a language model). Let \mathcal{V} be the token vocabulary of the underlying language model. There are K nodes; node $i \in \{1, \dots, K\}$ holds a local retrieval corpus $C_{i,t}$ and a local retrieval mechanism, and raw node-local data and corpora never leave their node. A global student model $\hat{P}^{(0)}$ is available at deployment start, typically obtained from a federated training stage; we use the *Federated Probe-Logit Distillation* (FPLD) protocol of [Dubey and Huo, 2026] as the running training stage, where each node fine-tunes locally and exchanges B -bit quantized logits on a shared probe set rather than gradients or weights. Theorem 1 of [Dubey and Huo, 2026] gives an explicit high-probability KL rate for FPLD in (K, n, m, B, V) , which we reuse as a black-box rate input for Theorem 4.12. During deployment, the active student is denoted \hat{P}_t and may be refreshed at selected intervention times.

Per-query protocol. At each time $t \in \mathbb{N}$, a query-answer pair $(X_t, Y_t) \in \mathcal{X} \times \mathcal{Y}$ is realized; the operator does not commit to a terminal time in advance, and may inspect, recalibrate, or escalate after every query. We assume *immediate label feedback* in the main formulation: the true answer Y_t becomes available before the next query arrives, so revealed labels drive the monitoring process. Arbitrarily delayed labels are deferred to future work. At time t , node i retrieves a top- $k_{i,t}$ passage set $Z_{i,t} = R_{i,t}(X_t, C_{i,t}; k_{i,t}) \subseteq C_{i,t}$; corpora may evolve slowly and are not shared across nodes. Bandwidth is the only resource

we charge, and we charge uplink only: at time t , node i uploads a $B_{i,t}$ -bit summary of its local scores; at calibration-refresh times $t \in \mathcal{T}_{\text{cal}}$, node i also uploads a compressed calibration summary within a total budget B_t^{cal} ; retraining inherits its cost from the underlying training protocol (e.g., FPLD). The per-query inference plus calibration cost is $\Gamma_t^{\text{comm}} = \sum_{i=1}^K B_{i,t} + B_t^{\text{cal}} \mathbf{1}\{t \in \mathcal{T}_{\text{cal}}\}$.

Given query X_t , node i forms a candidate list $A_{i,t}(X_t) \subseteq \mathcal{Y}$ and local nonconformity scores $s_{i,t}(y) = -\log \widehat{P}_t(y | X_t, Z_{i,t})$ for $y \in A_{i,t}(X_t)$, clipped to $[0, S_{\text{max}}]$. Node i uploads a compressed message $U_{i,t} = Q_{B_{i,t}}(\{(y, s_{i,t}(y)) : y \in A_{i,t}(X_t)\})$, the hub decodes $U_{i,t}$ into approximate scores $\widetilde{s}_{i,t}(y)$, and aggregates them. With $K_{t,y} = |\{i : y \in A_{i,t}(X_t)\}|$,

$$s_t^*(y) = \frac{1}{K_{t,y}} \sum_{i: y \in A_{i,t}(X_t)} s_{i,t}(y), \quad s_t^{\text{swarm}}(y) = \frac{1}{K_{t,y}} \sum_{i: y \in A_{i,t}(X_t)} \widetilde{s}_{i,t}(y),$$

where $s_t^{\text{swarm}}(y) = +\infty$ if $K_{t,y} = 0$. The first is the *oracle uncompressed* swarm score; the second is what the hub actually sees. Inheriting candidate-set inclusion (Assumption B2 of [Dubey and Huo, 2026]), every y in the test or calibration support lies in $\bigcap_{i=1}^K A_{i,t}(X_t)$, i.e., $K_{t,y} = K$ uniformly; the analysis lifts to general $K_{t,y}$ at the cost of y -dependent variance constants.

2.2 Calibration and filtration

We maintain a rolling labeled calibration buffer $\mathcal{D}_t^{\text{cal}} = \{(X_s, Y_s) : s \in I_t^{\text{cal}}\}$ with $n_{\text{cal},t} := |I_t^{\text{cal}}|$, where I_t^{cal} is a predictable index set (e.g. a sliding window of the most recent answered queries or a batched refresh buffer). At a refresh time $t \in \mathcal{T}_{\text{cal}}$, node i recomputes its local scores on $\mathcal{D}_t^{\text{cal}}$, compresses the resulting score summary into its allotted share of B_t^{cal} bits, and uploads it. Let q_t^* denote the *oracle conformal* threshold from the full uncompressed calibration scores, and \widehat{q}_t the threshold reconstructed from compressed node summaries; the swarm outputs the implemented prediction set $C_t(X_t) = \{y \in \mathcal{Y} : s_t^{\text{swarm}}(y) \leq \widehat{q}_t\}$ with miscoverage indicator $M_t = \mathbf{1}\{Y_t \notin C_t(X_t)\}$.

Let $\mathcal{F}_t = \sigma(X_{1:t}, Y_{1:t}, \widehat{P}_{0:t}, \{C_{i,1:t}\}_i, \{B_{i,1:t}\}_i, \{U_{i,1:t}\}_i, \widehat{q}_{1:t}, \mathcal{A}_{1:t})$ be the observable history, where \mathcal{A}_t is the intervention action at time t . A stopping time τ is any \mathcal{F}_t -adapted random time. The core modeling restriction is *predictability*: any bandwidth schedule, recalibration schedule, or retraining trigger used at time t is \mathcal{F}_{t-1} -measurable. This is what lets monitoring and intervention coexist without breaking validity.

2.3 Slack decomposition: $\Delta_{\text{FL},t}$, $\Delta_{\text{RAG},t}$, $\Delta_{\text{train},t}$

Three slack terms enter the per-step coverage bound: federated calibration, retrieval bandwidth, and training-side approximation. Each is \mathcal{F}_{t-1} -measurable by predictability of the associated schedule. We restate each at the level of detail required to follow the analysis of Section 4; full constructions and constants are in [Dubey and Huo, 2026].

Retrieval-bandwidth distortion ($\Delta_{\text{RAG},t}$). Inheriting Assumption (B3) of [Dubey and Huo, 2026], each node's QUANTIZESCORE primitive is a subtractively dithered scalar quantizer, so that the per-node quantized score decomposes additively as $\widetilde{s}_{i,t}(X_t, y) = s_{i,t}(X_t, y) + \xi_{i,t}(X_t, y)$, with $\{\xi_{i,t}\}_{i=1}^K$ conditionally independent across nodes given (\mathcal{F}_{t-1}, X_t) , mean zero, and bounded conditional second moment $\mathbb{E}[\xi_{i,t}^2 | \mathcal{F}_{t-1}, X_t] \leq v(B_{i,t})$ where $v(B) = O(2^{-2B/b_s})$ for a protocol-specific scale b_s . By the average-aggregation

rule, the implemented swarm score satisfies $s_t^{\text{swarm}}(X_t, y) = s_t^*(X_t, y) + \bar{\xi}_t(X_t, y)$ with $\bar{\xi}_t := (1/K) \sum_i \xi_{i,t}$, and cross-node independence yields $\mathbb{E}[\bar{\xi}_t^2 \mid \mathcal{F}_{t-1}, X_t] \leq V_{K,t} := (1/K^2) \sum_i v(B_{i,t})$. Combined with the $f_{\max,t}$ -Lipschitz score CDF (Assumption 4.3, (B5')) and Cauchy–Schwarz on $\mathbb{E}|\bar{\xi}_t| \leq \sqrt{V_{K,t}}$, the per-step retrieval-bandwidth slack is

$$\Delta_{\text{RAG},t} = f_{\max,t} \sqrt{\frac{1}{K^2} \sum_{i=1}^K v(B_{i,t})}.$$

The $1/K^2$ averaging (rather than the worst-case $1/K$) is the variance gain from independent cross-node dithering.

Federated-calibration distortion ($\Delta_{\text{FL},t}$). The threshold \hat{q}_t deviates from the population $(1 - \alpha)$ -quantile q_t^{pop} via a deterministic compression piece $|\hat{q}_t - q_t^*| \leq \phi(B_t^{\text{cal}}) = O(2^{-B_t^{\text{cal}}/b_q})$ (e.g., a quantized order-statistics summary or a GC-FCP / Fed-CCP core-set [Wen et al., 2026, Xu et al., 2025]) and a statistical piece $|q_t^* - q_t^{\text{pop}}|$ from the i.i.d. buffer. To control the latter pointwise rather than only on average, we fix a summable per-step *calibration budget* $\{\delta_t^{\text{cal}}\}_{t \geq 1}$ with $\sum_{t \geq 1} \delta_t^{\text{cal}} \leq \delta_{\text{cal}} \in (0, 1)$; the canonical choice is $\delta_t^{\text{cal}} = 6\delta_{\text{cal}}/(\pi^2 t^2)$. Sub-Gaussian deviation of the empirical $(1 - \alpha)$ -quantile gives, with probability at least $1 - \delta_t^{\text{cal}}$,

$$|\hat{q}_t - q_t^{\text{pop}}| \leq c_q \sqrt{\log(2/\delta_t^{\text{cal}})/n_{\text{cal},t}} + \phi(B_t^{\text{cal}}), \quad (1)$$

for an absolute constant c_q . Pushing (1) through the score CDF yields

$$\Delta_{\text{FL},t} = f_{\max,t} \left(c_q \sqrt{\log(2/\delta_t^{\text{cal}})/n_{\text{cal},t}} + \phi(B_t^{\text{cal}}) \right). \quad (2)$$

The event G_t that (1) holds at time t is \mathcal{F}_{t-1} -measurable and has $\mathbb{P}(G_t) \geq 1 - \delta_t^{\text{cal}}$; the cumulative *cal-good* event $\Omega_{\text{cal}} := \bigcap_{t \geq 1} G_t$ satisfies $\mathbb{P}(\Omega_{\text{cal}}) \geq 1 - \delta_{\text{cal}}$. The conditional theorems below take the form “on G_t ” or “on Ω_{cal} ” and absorb δ_{cal} into the final probability budget. The conditional bound (2) is strictly weaker than the marginal-over-calibration form of [Dubey and Huo, 2026] Theorem 2 by a factor $\sqrt{\log(2/\delta_t^{\text{cal}})/\log(2/\delta_{\text{cal}})}$, which grows from $\approx 1.07 \times$ at $t = 1$ to $\approx 2.48 \times$ at $t = 10^4$ for $\delta_{\text{cal}} = 0.05$, a slow $O(\sqrt{\log t})$ price for converting marginal validity into pointwise-conditional validity.

Training-side distortion ($\Delta_{\text{train},t}$). Let $\varepsilon_{\text{train},t}$ denote the current training-side approximation level, an upper bound on $\mathbb{E}_X[\text{KL}(P^*(\cdot \mid X) \parallel \hat{P}_t(\cdot \mid X))]$, and let $\Delta_t(x, y) := s_t^*(x, y) - s_{\text{ideal}}^*(x, y) = \log(P^*(y \mid x)/\hat{P}_t(y \mid x))$ be the score-level training residual. The indicator-difference + FTC + Pinsker chain of [Dubey and Huo, 2026, Corollary 3], under the (B5') conditional-density clause inherited in Assumption 4.3, yields the two-term bound

$$\Delta_{\text{train},t} = f_{\max,t} (\varepsilon_{\text{train},t} + \sqrt{2\varepsilon_{\text{train},t}}).$$

In the small- $\varepsilon_{\text{train},t}$ regime (typical post-FPLD-training), the second summand dominates and recovers the Pinsker $\sqrt{\cdot}$ shape. Theorem 4.12 bounds $\varepsilon_{\text{train},t}$ via the FPLD rate at the most recent training event. Under adversarial models violating the conditional-density clause, only the weaker rate $\Delta_{\text{train},t} = O(f_{\max,t} \varepsilon_{\text{train},t}^{1/4})$ is recoverable via Markov truncation; we adopt the (B5') regime as the operating assumption.

The four slack objects entering the per-step coverage bound are summarized below.

| Symbol | Source of slack | Form |
|----------------------------|-----------------------------------------------|----------------------------------------------------------------------------------------------------------------|
| $1/(n_{\text{cal},t} + 1)$ | Discrete split-conformal overshoot | Vanishes as $n_{\text{cal},t} \rightarrow \infty$ |
| $\Delta_{\text{FL},t}$ | Federated calibration: quantile + compression | $f_{\max,t} \left(c_q \sqrt{\log(2/\delta_t^{\text{cal}})/n_{\text{cal},t}} + \phi(B_t^{\text{cal}}) \right)$ |
| $\Delta_{\text{RAG},t}$ | Retrieval-bandwidth quantization | $f_{\max,t} \sqrt{(1/K^2) \sum_i v(B_{i,t})}$ |
| $\Delta_{\text{train},t}$ | Distilled-student approximation (FTC + B5') | $f_{\max,t} (\varepsilon_{\text{train},t} + \sqrt{2\varepsilon_{\text{train},t}})$ |

2.4 The deployment null and scope

The base-paper FC-RAG inequality, lifted to a one-step conditional bound on the per-query miscoverage, is

$$\mathbb{E}[M_t \mid \mathcal{F}_{t-1}] \mathbf{1}_{G_t} \leq b_t \mathbf{1}_{G_t}, \quad b_t := \alpha + \frac{1}{n_{\text{cal},t} + 1} + \Delta_{\text{FL},t} + \Delta_{\text{RAG},t} + \Delta_{\text{train},t}. \quad (3)$$

We call (3) the *deployment null* H_0 . Each $\Delta_{\bullet,t}$ is \mathcal{F}_{t-1} -measurable by predictability, hence so is b_t . The bound holds pointwise on the calibration-good event G_t ; off G_t the bound is vacuous and the residual probability is absorbed into the final δ_{cal} budget. The theorems in Section 4 test whether the realized stream is consistent with H_0 on Ω_{cal} . The classical $1/(n_{\text{cal},t} + 1)$ split-conformal overshoot is included for compatibility with the marginal-coverage bound of [Dubey and Huo, 2026, Theorem 2] and is dominated by $\Delta_{\text{FL},t}$ for typical $n_{\text{cal},t}$.

Adversarial nodes, differential privacy, open-ended generation, arbitrarily delayed labels, and architecture-heterogeneous clients are excluded from the first version of the theory. Each is a natural extension, but none is necessary to formulate the sequential object above.

3 The Anytime-FC-RAG protocol

The protocol is synchronous, single-aggregator, and charges uplink communication only. Figure 1 shows the two coupled loops: a fast per-query inference loop in which K nodes serve a query under their bandwidth budgets, and a slow sequential-testing loop in which observed miscoverage drives a betting e-process and a predictable controller feeds back to budgets, threshold, and student.

Once the answer Y_t is observed, the hub computes $M_t = \mathbf{1}\{Y_t \notin C_t(X_t)\}$ and updates the betting e-process

$$E_0 = 1, \quad E_t = E_{t-1} (1 + \lambda_t Z_t), \quad Z_t := M_t - b_t, \quad (4)$$

where $\lambda_t \in [0, 1/b_t]$ is predictable. The bound $\lambda_t \leq 1/b_t$ ensures $1 + \lambda_t Z_t \geq 0$ on every realization, since $Z_t \geq -b_t$. The alarm time is

$$\tau_{\text{alarm}} = \inf\{t \geq 1 : E_t \geq 1/\delta\}.$$

Note the algorithm *does not reset* E_t after an alarm or refresh: E_t continues to accumulate evidence across interventions, which is what preserves the time-uniform Ville bound across the entire post-deployment trajectory. (A reset variant with budgeted δ across epochs is also valid; we discuss this in Section 4.5.) The ordering inside Algorithm 1 is essential: \hat{q}_t is set from \mathcal{F}_{t-1} *before* X_t is served, M_t is recorded, E_t is updated using \mathcal{F}_{t-1} -measurable

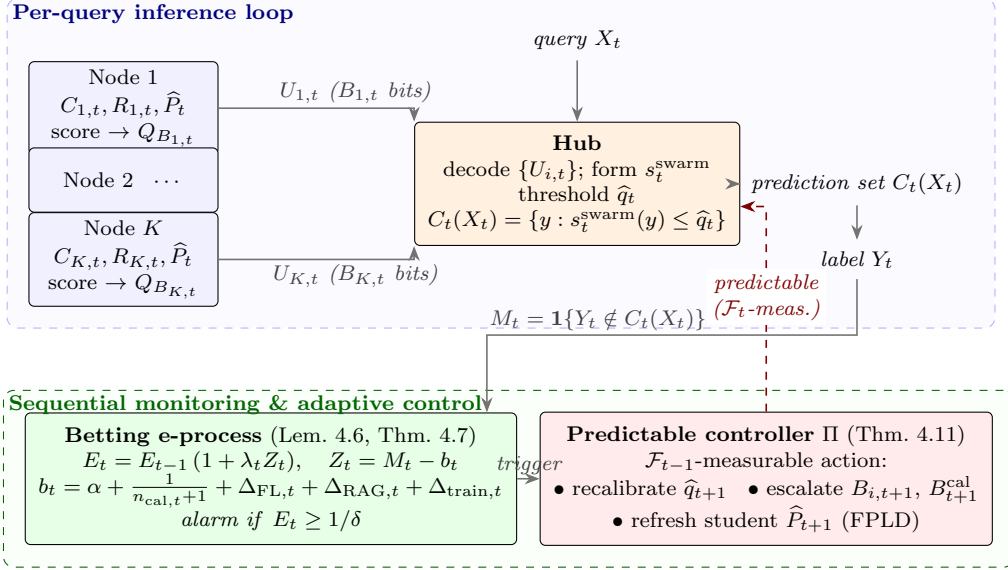


Figure 1: Anytime-FC-RAG architecture. **Top (blue)**: per-query inference loop: K nodes retrieve, score, and uplink $B_{i,t}$ -bit summaries; the hub assembles the conformal set $C_t(X_t)$. **Bottom (green)**: sequential monitoring loop: the betting e-process E_t tests the deployment null, and the predictable controller Π recalibrates, escalates bandwidth, or refreshes the student. All controller actions are \mathcal{F}_t -measurable (red dashed), preserving validity (Theorems 4.11, 4.9).

b_t and λ_t , and only *then* does the controller act, executing Algorithm 2 to recompute the threshold and choose the next round’s budgets. Each downstream object is therefore predictable with respect to the next round.

Predictable interventions. The controller may react to the monitoring state in three ways: (i) *recalibration* (request fresh compressed calibration summaries and update \hat{q}_t); (ii) *bandwidth escalation* (increase selected $B_{i,t}$ or the calibration-refresh budget B_t^{cal}); (iii) *retraining refresh* (replace the current student with a refreshed model). All such actions must be \mathcal{F}_{t-1} -measurable. That predictability condition is what lets the same e-process both guide interventions and remain valid after them (Theorem 4.11).

Relationship to FC-RAG. Fixed-horizon FC-RAG [Dubey and Huo, 2026] sits inside our framework as the degenerate case in which $B_{i,t} \equiv B_i$, the threshold \hat{q}_t is computed once from a one-shot calibration set, the student is frozen throughout deployment, no intervention is triggered, and only the terminal-time miscoverage matters. The bounds differ in conditioning structure: FC-RAG’s marginal-coverage Theorem 2 holds with high probability over the calibration draw, whereas the present paper’s per-step bound holds conditional on \mathcal{F}_{t-1} on the cal-good event G_t (with the residual probability collected into δ_{cal} via union bound). The new ingredients of Anytime-FC-RAG are exactly three: a *rolling* calibration state, a (*truncated*) *e-process* for time-uniform monitoring, and *predictable* control actions that change bandwidth or refresh the model only when justified by accumulated evidence.

Algorithm 1 Anytime-FC-RAG: query-time inference and monitoring

Require: Initial student $\widehat{P}^{(0)}$; initial threshold \widehat{q}_0 ; target level α ; alarm level δ ; predictable controller Π ; per-node budgets $\{B_{i,1}\}_{i=1}^K$; betting cap $\bar{\lambda}$.

```
1:  $E_0 \leftarrow 1$ 
2: for  $t = 1, 2, \dots$  do
3:   Hub broadcasts query  $X_t$  to all nodes
4:   for each node  $i = 1, \dots, K$  in parallel do
5:      $Z_{i,t} \leftarrow R_{i,t}(X_t, C_{i,t}; k_{i,t})$ 
6:      $A_{i,t}(X_t) \leftarrow \text{TOPCANDIDATES}(\widehat{P}_t(\cdot | X_t, Z_{i,t}))$ 
7:      $s_{i,t}(y) \leftarrow -\log \widehat{P}_t(y | X_t, Z_{i,t})$  for  $y \in A_{i,t}(X_t)$ 
8:      $U_{i,t} \leftarrow Q_{B_{i,t}}(\{(y, s_{i,t}(y)) : y \in A_{i,t}(X_t)\})$ 
9:     Uplink  $U_{i,t}$  to hub
10:  end for
11:  Hub decodes  $\{U_{i,t}\}_{i=1}^K$ , forms  $s_t^{\text{swarm}}$ , and sets  $C_t(X_t) \leftarrow \{y \in \mathcal{Y} : s_t^{\text{swarm}}(y) \leq \widehat{q}_t\}$ 
12:  Observe label  $Y_t$ , set  $M_t \leftarrow \mathbf{1}\{Y_t \notin C_t(X_t)\}$ ,  $Z_t \leftarrow M_t - b_t$ 
13:  Choose predictable  $\lambda_t \in [0, \min(\bar{\lambda}, 1/b_t)]$  from  $\mathcal{F}_{t-1}$ 
14:   $E_t \leftarrow E_{t-1} (1 + \lambda_t Z_t)$ 
15:  Update rolling buffer  $\mathcal{D}_t^{\text{cal}} \leftarrow \text{BUFFERUPDATE}(\mathcal{D}_{t-1}^{\text{cal}}; (X_t, Y_t))$ 
16:  if  $E_t \geq 1/\delta$  or  $\Pi(\mathcal{F}_t)$  requests refresh then
17:    Execute Algorithm 2 ▷ predictable intervention;  $E_t$  continues, not reset
18:  end if
19: end for
```

Algorithm 2 REFRESHTHRESHOLDANDCONTROL

Require: History \mathcal{F}_t ; rolling calibration buffer $\mathcal{D}_t^{\text{cal}}$; calibration budget B_t^{cal}

```
1: for each node  $i = 1, \dots, K$  in parallel do
2:   Recompute local scores on  $\mathcal{D}_t^{\text{cal}}$  using current  $\widehat{P}_t$  and local retrieval
3:    $S_{i,t}^{\text{cal}} \leftarrow \text{COMPRESSCALSUMMARY}_i(\mathcal{D}_t^{\text{cal}}; B_t^{\text{cal}})$ 
4:   Uplink  $S_{i,t}^{\text{cal}}$  to hub
5: end for
6: Hub reconstructs updated threshold  $\widehat{q}_{t+1}$  from  $\{S_{i,t}^{\text{cal}}\}_{i=1}^K$ 
7: Predictably choose next budgets  $\{B_{i,t+1}\}_{i=1}^K$  and retrieval settings from  $\mathcal{F}_t$ 
8: if  $\Pi(\mathcal{F}_t)$  declares model-side drift then
9:   Refresh student  $\widehat{P}_{t+1}$  via FPLD or another approved training stage
10: else
11:    $\widehat{P}_{t+1} \leftarrow \widehat{P}_t$ 
12: end if
```

4 Anytime-valid guarantees

Off-the-shelf sequential testing supplies Ville’s inequality and the Hoeffding-stitched envelope, and base FC-RAG [Dubey and Huo, 2026] supplies the slack decomposition $\Delta_{\text{FL},t}, \Delta_{\text{RAG},t}, \Delta_{\text{train},t}$ in marginal-over-calibration form. Neither composes into a sound conditional supermartingale on its own, because base FC-RAG’s coverage bound is a marginal claim (it fails conditionally on adverse calibration realizations) and the betting e-process needs a strict conditional centering. Our load-bearing construction is the *cal-deviation budget* $\{\delta_t^{\text{cal}}\}$ together with the resulting calibration-good event G_t and the *truncated supermartingale* $\tilde{E}_t = E_t \mathbf{1}_{\cap_{s \leq t} G_s}$: this is what converts the marginal slack form into a strict conditional bound (Lemma 4.5) and turns the obstructed e-process into a bona fide supermartingale on the entire probability space (Lemma 4.6). Once those two pieces are in place, the rest is reuse: Ville’s inequality (Theorem 4.7), Hoeffding-stitching (Theorem 4.9), predictability of the controller (Theorem 4.11), and the FTC + (B5’) chain of [Dubey and Huo, 2026, Corollary 3] applied to the FPLD KL rate (Theorem 4.12).

The analysis is organized in six results. Lemma 4.5 lifts the base-paper Theorem 2 to a one-step conditional bound on G_t . Lemma 4.6 establishes that \tilde{E}_t is a nonnegative supermartingale. Theorem 4.7 applies Ville’s inequality and a union bound on G_t to recover a time-uniform alarm guarantee. Theorem 4.9 converts the same construction into a time-uniform envelope on cumulative miscoverage. Theorem 4.11 shows that predictable interventions preserve both guarantees. Theorem 4.12 bounds $\Delta_{\text{train},t}$ using the FPLD training rate at the most recent refresh.

4.1 Assumptions

Assumption 4.1 (Predictable schedules). *For every t , the calibration index set I_t^{cal} , the budgets $\{B_{i,t}\}_{i=1}^K$ and B_t^{cal} , the active student \hat{P}_t , the threshold \hat{q}_t , the slack quantities b_t , and the betting fraction λ_t are all \mathcal{F}_{t-1} -measurable.*

Assumption 4.2 (I.i.d. data and predictable buffer). *The deployment sequence $(X_t, Y_t)_{t \geq 1}$ is i.i.d. from a fixed joint law \mathcal{P} on $\mathcal{X} \times \mathcal{Y}$, and for every t the calibration index set satisfies $I_t^{\text{cal}} \subseteq \{1, \dots, t-1\}$ and is \mathcal{F}_{t-1} -measurable.*

This is the analogue of Assumption (B1) in [Dubey and Huo, 2026], adapted to the sequential setting. It is the cleanest sufficient condition for the per-step rank exchangeability between (X_t, Y_t) and the buffer points to drive the conditional coverage analysis below; the buffer, being \mathcal{F}_{t-1} -measurable, is held fixed when conditioning, and randomness reduces to the test point and the buffer realization (the latter shared between \mathcal{F}_{t-1} and the implicit G_t event over the buffer draw). The assumption fails under genuine drift, and rejection of the deployment null is exactly the alarm event the e-process detects.

Assumption 4.3 (Bounded score and strengthened density regularity). *The score s is bounded in $[0, S_{\max}]$ (clipping). The cumulative distribution function F_t of the oracle uncompressed score $s_t^*(X_t, Y_t)$ admits a density $f_t \leq f_{\max,t}$ on a fixed deterministic neighborhood $[q_t^{\text{pop}} - r_t, q_t^{\text{pop}} + r_t]$ for some $r_t > 0$; the analysis verifies a posteriori via (1) that \hat{q}_t lies inside this neighborhood with probability at least $1 - \delta_t^{\text{cal}}$. Inheriting (B5’) of [Dubey and Huo, 2026], the conditional density (on the same neighborhood) of the relevant “before-perturbation” score given the perturbation is also bounded by $f_{\max,t}$ in two specific cases:*

- Retrieval-bandwidth dither (Step 3 of Lemma 4.5): the conditional density of $s_t^*(X_t, Y_t)$ given the dither average $\bar{\xi}_t(X_t, Y_t) := (1/K) \sum_i \xi_{i,t}(X_t, Y_t)$, where $\bar{\xi}_t$ has $\mathbb{E}[\bar{\xi}_t | \mathcal{F}_{t-1}, X_t] = 0$ and bounded conditional second moment by Assumption (B3) of [Dubey and Huo, 2026].
- Training residual (FTC chain of Section 2 and Theorem 4.12): the conditional density of $s_{\text{ideal}}^*(X_t, Y_t) := -\log P^*(Y_t | X_t)$ given $\Delta_t(X_t, Y_t) := \log(P^*(Y_t | X_t)/\hat{P}_t(Y_t | X_t)) = s_t^* - s_{\text{ideal}}^*$.

Assumption 4.4 (Slack admissibility). For every t , $b_t \in (0, 1 - \eta]$ for some fixed $\eta > 0$, and the betting cap $\bar{\lambda}$ satisfies $\bar{\lambda} \leq 1/b_t$ uniformly in t .

Assumption 4.4 ensures the e-process stays nonnegative; we typically take $\bar{\lambda} \leq 1/(\alpha + \Delta_{\max})$ for a slack upper bound Δ_{\max} chosen by the operator.

4.2 One-step deployment null

Lemma 4.5 (One-step deployment null on the cal-good event). Under Assumptions 4.1–4.3, on the calibration-good event G_t defined in Section 2 (which satisfies $\mathbb{P}(G_t) \geq 1 - \delta_t^{\text{cal}}$),

$$\mathbb{E}[M_t | \mathcal{F}_{t-1}] \mathbf{1}_{G_t} \leq b_t \mathbf{1}_{G_t}.$$

Equivalently, on the event G_t , $\mathbb{E}[M_t | \mathcal{F}_{t-1}] \leq b_t$.

Proof. The proof is provided in Appendix S1.1. □

This is the conditional bound the betting e-process needs as a supermartingale on top of FC-RAG. The pointwise form on G_t (not FC-RAG’s marginal Theorem 2 form) is the centering Ville’s inequality requires; without it, no anytime-valid alarm is possible. The price is a $\sqrt{\log(2/\delta_t^{\text{cal}})}$ inflation of $\Delta_{\text{FL},t}$, an $O(\sqrt{\log t})$ factor amounting to $1.07 \times -2.72 \times$ across $t \in [1, 10^5]$. The cal-deviation budget is not optional: without it, the marginal centering fails the supermartingale property on adverse calibration draws and Ville’s inequality cannot be applied (Appendix S1).

4.3 Alarm validity

Define the per-step centered residual $Z_t := M_t - b_t \in [-b_t, 1 - b_t]$, an \mathcal{F}_t -measurable bounded random variable, and the cumulative cal-good event $\Omega_{\text{cal},t} := \bigcap_{s \leq t} G_s$ (\mathcal{F}_{t-1} -measurable since each G_s is \mathcal{F}_{s-1} -measurable).

Lemma 4.6 (Truncated e-process is a supermartingale). Under Lemma 4.5 and Assumptions 4.1, 4.4, define the truncated e-process

$$\tilde{E}_t := E_t \cdot \mathbf{1}_{\Omega_{\text{cal},t}}, \quad \tilde{E}_0 := 1,$$

where E_t is the betting e-process (4) with predictable $\lambda_t \in [0, 1/b_t]$. Then $(\tilde{E}_t)_{t \geq 0}$ is a nonnegative supermartingale with $\mathbb{E}\tilde{E}_0 = 1$:

$$\mathbb{E}[\tilde{E}_t | \mathcal{F}_{t-1}] \leq \tilde{E}_{t-1} \quad \text{for every } t \geq 1.$$

Proof. The proof is provided in Appendix S1.2. □

Theorem 4.7 (Time-uniform alarm validity). *Under the assumptions of Lemma 4.6, for every $\delta_e \in (0, 1)$,*

$$\mathbb{P}\left(\sup_{t \geq 1} E_t \geq 1/\delta_e\right) \leq \delta_e + \delta_{\text{cal}}.$$

In particular, with the canonical split $\delta_e = \delta_{\text{cal}} = \delta/2$, the alarm time $\tau_{\text{alarm}} = \inf\{t : E_t \geq 2/\delta\}$ satisfies $\mathbb{P}(\tau_{\text{alarm}} < \infty \mid H_0) \leq \delta$.

Proof. The proof is provided in Appendix S1.3. □

Remark 4.8 (Total probability budget). *Theorem 4.7's budget $\delta_e + \delta_{\text{cal}}$ holds on the training-good event of Theorem 4.12, which has probability $\geq 1 - \delta_{\text{train}}$ over the training draws. Combining by union bound, the unconditional alarm guarantee is $\mathbb{P}(\sup_t E_t \geq 1/\delta_e) \leq \delta_e + \delta_{\text{cal}} + \delta_{\text{train}}$, matching the user-facing total stated in Section 1. The canonical equal split $\delta_e = \delta_{\text{cal}} = \delta_{\text{train}} = \delta/3$ recovers a single δ -level guarantee.*

4.4 Cumulative-miscoverage envelope

The alarm at $\sup_t E_t \geq 1/\delta$ controls the probability of *ever* flagging a violation. To get a numerically interpretable coverage statement at any predictable stopping time τ we use the cumulative residual.

Theorem 4.9 (Time-uniform Hoeffding envelope). *Under Lemma 4.5 and Assumption 4.1, define $S_t := \sum_{s=1}^t (M_s - b_s) = \sum_{s=1}^t Z_s$. Then $|Z_s| \leq 1$ deterministically, and for every $\delta_e \in (0, 1)$ there is an explicit boundary $u_t(\delta_e)$ with*

$$\mathbb{P}(\exists t \geq 1 : S_t > u_t(\delta_e)) \leq \delta_e + \delta_{\text{cal}}.$$

A closed-form admissible choice (polynomial-stitching variant of [Howard et al., 2021]) is

$$u_t(\delta_e) = c_H \sqrt{\frac{1}{2} t \left(\log(1/\delta_e) + \log(1 + \log_2 t) \right)}$$

with absolute constant $c_H \leq 1.7$. In particular, with probability at least $1 - \delta_e - \delta_{\text{cal}}$, for every stopping time τ adapted to (\mathcal{F}_t) ,

$$\frac{1}{\tau} \sum_{s=1}^{\tau} M_s \leq \alpha + \frac{1}{\tau} \sum_{s=1}^{\tau} \left(\frac{1}{n_{\text{cal},s}+1} + \Delta_{\text{FL},s} + \Delta_{\text{RAG},s} + \Delta_{\text{train},s} \right) + \frac{u_{\tau}(\delta_e)}{\tau}.$$

The envelope width $u_{\tau}(\delta_e)/\tau = O(\sqrt{\log \log \tau/\tau})$ vanishes with τ .

Proof. The proof is provided in Appendix S1.4. □

Remark 4.10. *The envelope and the betting e-process are complementary: E_t accumulates evidence multiplicatively and is best when violations are persistent (high power for sustained drift), while $u_t(\delta)$ controls the cumulative deviation at any finite horizon and is best for reporting an interpretable upper bound on the realized miscoverage rate. We track both and report whichever is tighter at the requested δ .*

4.5 Safe adaptive control

Theorem 4.11 (Safe adaptive control). *Let Π be any controller that maps \mathcal{F}_{t-1} to a (possibly randomized) action in \mathcal{A}_t , where \mathcal{A}_t ranges over: recalibration refreshes (changing \hat{q}_t), per-node bandwidth changes (changing $B_{i,t}$ or B_t^{cal}), and student refreshes (changing \hat{P}_t). If every action is \mathcal{F}_{t-1} -measurable, then under Assumptions 4.1–4.4 the supermartingale property of the truncated e -process (\tilde{E}_t) and the time-uniform Hoeffding envelope of Theorem 4.9 both continue to hold. Hence the alarm bound $\mathbb{P}(\sup_t E_t \geq 1/\delta_e) \leq \delta_e + \delta_{\text{cal}}$ of Theorem 4.7 and the envelope bound of Theorem 4.9 apply to the controlled trajectory.*

Proof. The proof is provided in Appendix S1.5. \square

Sticky vs. resetting alarms. Algorithm 1 does not reset E_t after an alarm (sticky mode). A reset variant with per-epoch budgets is also valid; both variants preserve Theorem 4.7 (Appendix S1).

4.6 Training propagation

Theorem 4.12 (Training propagation under (B5')). *Fix a summable per-training-event budget $\{\delta_r\}_{r \geq 1}$ with $\sum_{r \geq 1} \delta_r \leq \delta_{\text{train}}$ (canonical choice $\delta_r = 6\delta_{\text{train}}/(\pi^2 r^2)$). Suppose the student \hat{P}_t used at deployment time t comes from FPLD training event $r(t)$ [Dubey and Huo, 2026, Theorem 1] with parameters $(K, n_{r(t)}, m_{r(t)}, B_{r(t)}, V)$, and let*

$$\mathcal{R}_{r(t)} := \frac{c_1 d}{K n_{r(t)}} + c_2 \rho \frac{V \log(V/\delta_{r(t)})}{\sqrt{m_{r(t)}}} + c_3 2^{-2B_{r(t)}/V} + \varepsilon_{\text{opt}} + \varepsilon_{\text{fit}}$$

denote the corresponding training-rate bound. Under the strengthened conditional-density clause of Assumption 4.3, with probability at least $1 - \delta_{\text{train}}$ over the training draws, simultaneously over all $t \geq 1$,

$$\Delta_{\text{train},t} \leq f_{\text{max},t} (\mathcal{R}_{r(t)} + \sqrt{2\mathcal{R}_{r(t)}}).$$

Proof. The proof is provided in Appendix S1.6. \square

In the small- \mathcal{R} regime the $\sqrt{2\mathcal{R}_{r(t)}}$ summand dominates, recovering the Pinsker shape. Absent (B5'), only the weaker $O(\mathcal{R}^{1/4})$ rate is recoverable; the sequential-testing layer is unaffected either way (Appendix S1).

Open direction. A communication-optimality oracle inequality of the form $\mathbb{E} \sum_{t=1}^T \Gamma_t^\Pi \leq \inf_{\Pi' \in \mathfrak{C}_{\text{valid}}} \mathbb{E} \sum \Gamma_t^{\Pi'} + \text{overhead}(T)$, where $\mathfrak{C}_{\text{valid}}$ is the class of validity-preserving controllers, would be substantially stronger than Theorem 4.11. We do not attempt it here and flag it as future work.

5 Experiments

The experiments split into two qualitatively distinct roles. *Synthetic experiments* probe the sequential-testing layer in isolation on Bernoulli streams whose conditional miscoverage is set by hand, decoupled from the FC-RAG / FPLD pipeline. *Real-world experiments* deploy the GPT-2-small + MiniLM swarm of [Dubey and Huo, 2026, §7.5] on three benchmarks

— MMLU [Hendrycks et al., 2021] (in-cal-set redistribution), DBpedia ontology [Lehmann et al., 2015] (drift to a class the swarm has no node for), and AG News [Zhang et al., 2015] (drift to a target recoverable from GPT-2 priors) — and compare against conformal test martingales [Vovk et al., 2021], CUSUM, Shiryaev–Roberts, and online conformal prediction [Angelopoulos et al., 2024b]. Real-world runs use 3 calibration splits \times 5 deployment seeds (15 trajectories per benchmark); synthetic runs use 200–2000 seeds. All runs use $\alpha = 0.10$, $\delta_e = 0.05$, $\delta_{\text{cal}} = 0.05$; per-experiment details and expanded ablations are in Appendix S2.

5.1 Sequential-testing layer validation

On synthetic Bernoulli streams, Type-I rate is 0.0105 at the boundary of H_0 and 0.0025 in the interior, both an order of magnitude below the $\delta_e + \delta_{\text{cal}} = 0.10$ budget (Table 2). Detection power saturates at $\geq 99.6\%$ from drift $+0.04$ onward, with median delay $3047 \rightarrow 687$ steps as drift grows from $+0.04$ to $+0.15$ (Figure 2, Table 3), matching the predicted $\Omega(\log \log T/\text{drift}^2)$ rate. The Hoeffding-stitched envelope holds across all 4000 null trajectories with 0.0000 breach rate, and a Monte-Carlo sanity check confirms Lemma 4.5 pointwise (Appendix S2.1).

Table 2: Type-I rate is an order of magnitude below the $\delta_e + \delta_{\text{cal}} = 0.10$ budget on synthetic Bernoulli streams. $T = 5000$, 2000 seeds per regime.

| Regime | alarm rate | median $\sup_t E_t$ | $p_{95} \sup_t E_t$ | $p_{99} \sup_t E_t$ |
|--------------------------------------------------------|------------|---------------------|---------------------|---------------------|
| Boundary ($\mathbb{E}[Z_t \mathcal{F}_{t-1}] = 0$) | 0.0105 | 1.131 | 6.381 | 21.230 |
| Interior ($\mathbb{E}[Z_t \mathcal{F}_{t-1}] < 0$) | 0.0025 | 1.000 | 3.063 | 6.622 |

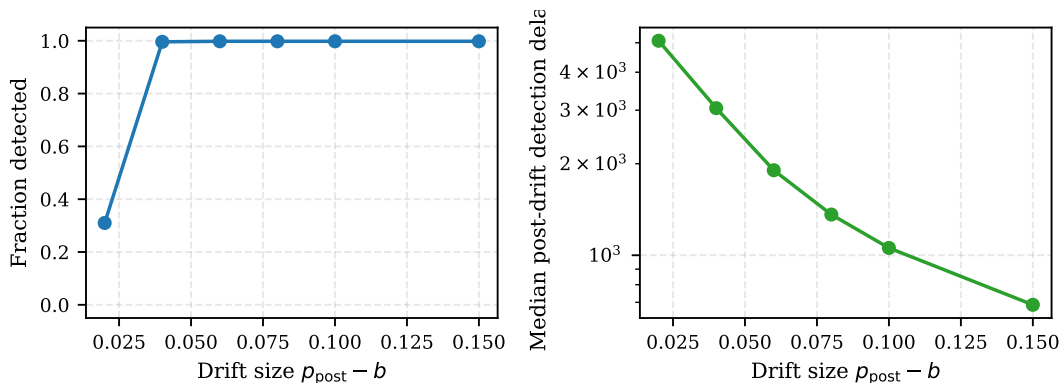


Figure 2: Detection saturates at $\geq 99.6\%$ by drift $+0.04$, with delay decaying log-linearly from ~ 5000 steps at $+0.02$ to ~ 700 at $+0.15$.

5.2 Slack decomposition and cost overhead

Empirical Δ_{RAG} tracks the variance form on a log-log axis with slope exactly -0.5000 for $K \in \{1, \dots, 128\}$ (Figure 3, left). The training slack’s two-term form holds tightly: empirical-to-theory ratio ≤ 0.91 (mean 0.65) across 20 Bernoulli pairs with Beta(2, 2) residuals. The cost-overhead factor $R(t)$ grows from 1.07 at $t = 1$ to only 2.72 at $t = 10^5$ (Figure 3, right), so the conditional construction is essentially free at any practical horizon.

Table 3: Delay decays inversely with drift size, matching the nonparametric $\Omega(\log \log T/\text{drift}^2)$ lower bound. Post-drift steps until $E_t \geq 1/\delta_e$; $T = 8000$, drift onset $t = 2000$, 500 seeds.

| Drift size | fraction detected | median delay | p_{95} delay |
|------------|-------------------|--------------|----------------|
| +0.02 | 0.310 | 5076 | 5938 |
| +0.04 | 0.996 | 3047 | 4464 |
| +0.06 | 0.998 | 1904 | 2685 |
| +0.08 | 0.998 | 1361 | 1864 |
| +0.10 | 0.998 | 1057 | 1480 |
| +0.15 | 0.998 | 687 | 931 |

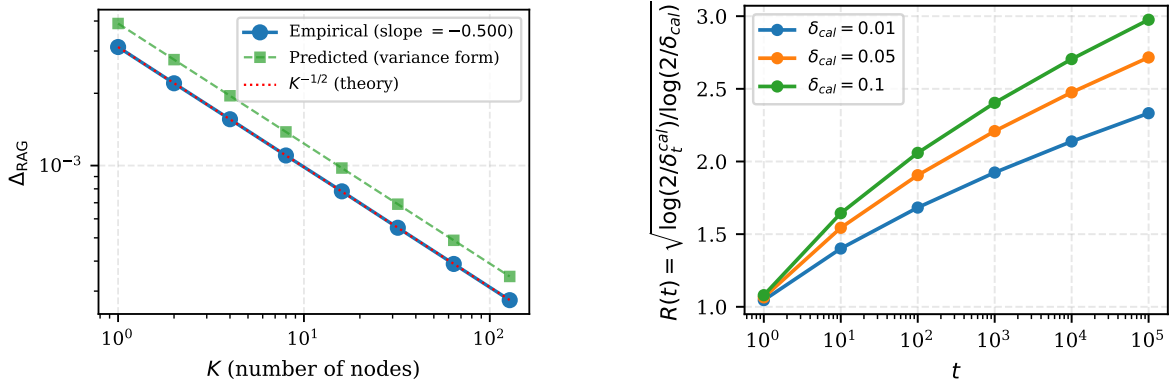


Figure 3: The slack decomposition is numerically tight and the conditional construction is essentially free. **Left:** Δ_{RAG} vs. K matches the theoretical $-1/2$ slope exactly. **Right:** cost-overhead $R(t) \leq 2\times$ at all practical horizons, growing only logarithmically.

Additional necessity checks (cal-deviation budget, predictability of the controller layer) and robustness studies (aGRAPA vs. constant- λ bettors, hyperparameter sensitivity) are reported in Appendix S2.4.

5.3 Adaptive bandwidth controller

On a synthetic stream with +0.20 drift at $t = 2500$, all three bandwidth regimes (low-only, high-only, adaptive) reach 100% alarm rate, but the adaptive regime pays only 1.708 on average — a 57% cost saving (Table 4). On the GPT-2-small swarm ($B_i = 8$ low, $B_i = 12$ high), the same pattern holds: on DBpedia all three regimes alarm at 100% and adaptive saves 14% (41.5 vs. 48.0); on MMLU and AG News (no genuine drift) the controller correctly does not escalate (Figure 4). Predictable escalation is a real operational lever: alarm validity is preserved, and high bandwidth is paid only where needed.

5.4 End-to-end real-world deployment and comparisons

The end-to-end result (Figure 5, Table 5) on the GPT-2-small + MiniLM swarm with sudden drift at $t = 500$ over $T = 2000$ (15 trajectories): the e-process is silent on MMLU in-cal redistribution (alarm 0.00, post-miscov 0.149) and AG News priors-recoverable drift (0.00, 0.127), and fires on DBpedia genuine drift (0.33, rising to 1.00 in the head-to-head;

Table 4: Adaptive controller saves 57% cost at identical 100% alarm rate. Drift $+0.20$ injected at $t = 2500$; $T = 5000$, 200 seeds.

| Regime | mean cost | alarm rate |
|---------------------------------------------|-----------|------------|
| Low only ($\Delta_{\text{RAG}} = 0.04$) | 1.000 | 1.000 |
| High only ($\Delta_{\text{RAG}} = 0.005$) | 4.000 | 1.000 |
| Adaptive ($0.5/\delta_e$ warning trigger) | 1.708 | 1.000 |

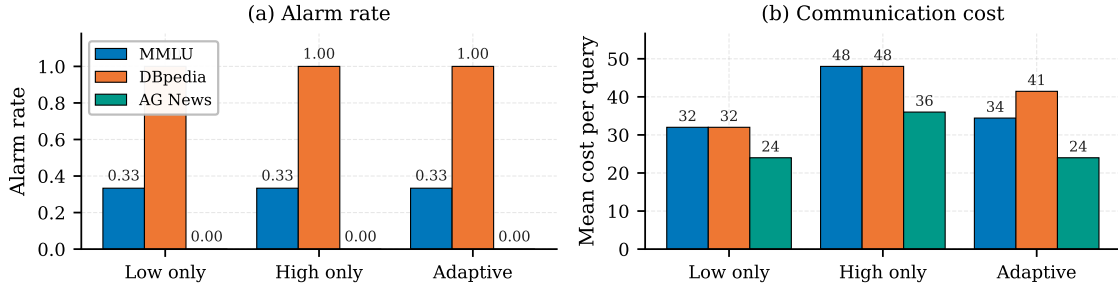


Figure 4: Adaptive controller (Theorem 4.11). All three bandwidth regimes match in alarm rate; the adaptive regime saves 14% of communication cost on DBpedia (41.5 vs. 48.0) without sacrificing detection.

post-miscov $0.370 > b \approx 0.21$). Three robustness ablations (drift schedule, heterogeneous bandwidth, FPLD multi-refresh) preserve this discriminative behavior (Appendix S2.3).

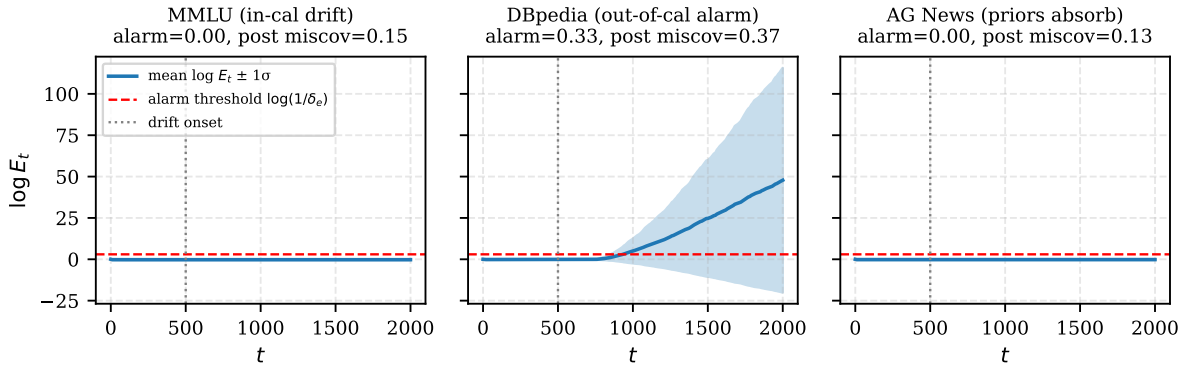


Figure 5: The alarm fires when and only when coverage genuinely breaks. Trajectory of $\log E_t$ on the GPT-2-small + MiniLM swarm under sudden drift at $t = 500$: silent on MMLU and AG News, fires on DBpedia.

Against prior monitoring methods, our e-process matches conformal test martingales [Vovk et al., 2021] in null validity (0.009 vs. 0.000) and dominates on drift (1.000 vs. 0.000 on large drift), because CTM does not exploit the slack-decomposed null bound. Parametric CUSUM and Shiryaev–Roberts match or exceed at every drift by assuming the alternative is known; our nonparametric e-process is slower only at borderline drift, the expected price of distribution-free testing [Howard et al., 2021, §6]. Online conformal [Angelopoulos et al., 2024b] adapts α_t to maintain coverage rather than alarming, so the two are complementary.

The real-world head-to-head makes this concrete (Figure 6): on DBpedia our alarm fires in every trajectory while OC compresses α_t from 0.10 to 0.031; on MMLU and AG News both heads correctly stay quiet. Aggregated (Table 5), the alarm fires when and only when coverage genuinely breaks.

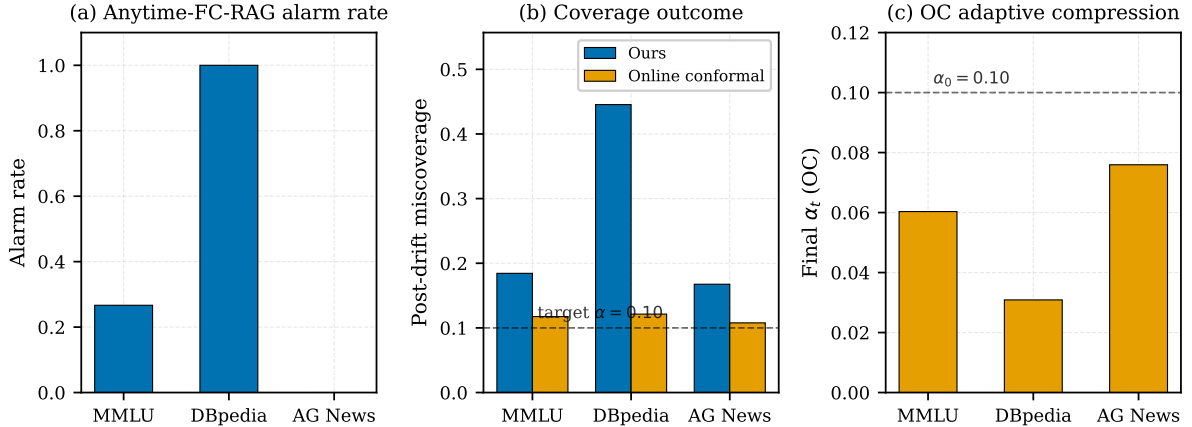


Figure 6: Head-to-head with online conformal [Angelopoulos et al., 2024b]. On DBpedia our alarm fires in every trajectory while OC compresses α_t from 0.10 to 0.031 to maintain coverage; on MMLU and AG News both methods correctly stay quiet. The two heads are complementary: ours surfaces events, OC adjusts set sizes.

Table 5: The alarm fires when and only when coverage genuinely breaks. Each cell reports alarm rate / mean post-drift miscoverage (or alarm rate / mean cost-per-query for the adaptive controller). The end-to-end row uses 15 trajectories; the head-to-head uses a paired configuration with higher power, hence DBpedia 1.00 vs. 0.33.

| Experiment | MMLU | DBpedia | AG News |
|-------------------------------|--------------|--------------|--------------|
| End-to-end | 0.00 / 0.149 | 0.33 / 0.370 | 0.00 / 0.127 |
| Sudden-drift ablation | 0.33 | 1.00 | 0.00 |
| Adaptive controller | 0.33 / 34.4 | 1.00 / 41.5 | 0.00 / 24.0 |
| Online-conformal head-to-head | 0.27 / 0.184 | 1.00 / 0.445 | 0.00 / 0.168 |

6 Discussion and outlook

Related work and what is new. Anytime-valid testing via e-processes goes back to [Ville, 1939] and was modernized for nonparametric settings in [Howard et al., 2020, 2021]; the betting interpretation we use [Waudby-Smith and Ramdas, 2024, Ramdas et al., 2023] and recent conformal extensions [Gauthier et al., 2025, Hultberg et al., 2026, Angelopoulos et al., 2024a, Gibbs and Candes, 2021, Angelopoulos et al., 2024b] cover the sequential-testing layer. The alarm half of our construction is a federated, bandwidth-aware analogue of conformal test martingales [Vovk et al., 2021]; classical CUSUM and Shiryaev–Roberts changepoint detection are recovered as the special case $b_t = \alpha$ of our construction. Single-site conformal-RAG [Li et al., 2024, Chakraborty

et al., 2026] and federated conformal prediction [Lu et al., 2023, Plassier et al., 2023, Wen et al., 2026, Xu et al., 2025] are proper subsets of our setting in distinct dimensions: the former assumes one model, one corpus, one calibration set; the latter takes the score as given and is silent on per-node retrieval bandwidth. Closest in spirit to our deployment null is the non-exchangeable coverage analysis of [Barber et al., 2023]. The construction is not RAG-specific: any sequential conformal protocol with i.i.d. deployment data, an \mathcal{F}_{t-1} -measurable threshold satisfying a high-probability quantile bound, and a predictable slack decomposition admits the same alarm and envelope guarantees at budget $\delta_e + \delta_{\text{cal}}$.

Summary. We extended FC-RAG from a fixed-horizon coverage guarantee to an anytime-valid deployment-time reliability framework via the cal-deviation budget and the truncated supermartingale; the four theorems cover alarm validity, cumulative-miscoverage envelope, safe adaptive control, and training-to-deployment propagation, and the empirical Type-I rate, detection power, envelope coverage, controller-cost saving, and discriminative real-LM behavior all match the predicted regimes (Section 5).

Limitations and broader impact. The main formulation assumes immediate label feedback, and switching to an empirical-Bernstein boundary [Howard et al., 2021] would tighten the envelope by typically $1.5\times$. Under adversarial models that violate the (B5') clause, only the weaker $\Delta_{\text{train},t} = O(f_{\text{max},t} \mathcal{R}_{r(t)}^{1/4})$ rate is recoverable; the sequential-testing layer is unaffected. The construction is not specific to RAG and can be attached to any sequential conformal protocol with a predictable slack decomposition. Two operational caveats: the conformal coverage guarantee holds in expectation across queries, not conditionally per input; and the protocol does not provide differential privacy on its own. Adversarial nodes, open-ended generation, architecture-heterogeneous clients, and a communication-optimality oracle inequality are out of scope.

References

- Anastasios Angelopoulos, Stephen Bates, Adam Fisch, Lihua Lei, and Tal Schuster. Conformal risk control. In B. Kim, Y. Yue, S. Chaudhuri, K. Fragkiadaki, M. Khan, and Y. Sun, editors, *International Conference on Learning Representations*, volume 2024, pages 55198–55218, 2024a. URL https://proceedings.iclr.cc/paper_files/paper/2024/file/f3549ef9b5ff520a7e41ff3cc306ab2b-Paper-Conference.pdf.
- Anastasios Nikolas Angelopoulos, Rina Barber, and Stephen Bates. Online conformal prediction with decaying step sizes. In Ruslan Salakhutdinov, Zico Kolter, Katherine Heller, Adrian Weller, Nuria Oliver, Jonathan Scarlett, and Felix Berkenkamp, editors, *Proceedings of the 41st International Conference on Machine Learning*, volume 235 of *Proceedings of Machine Learning Research*, pages 1616–1630. PMLR, 21–27 Jul 2024b. URL <https://proceedings.mlr.press/v235/angelopoulos24a.html>.
- Rina Foygel Barber, Emmanuel J. Candès, Aaditya Ramdas, and Ryan J. Tibshirani. Conformal prediction beyond exchangeability. *The Annals of Statistics*, 51(2):816 – 845, 2023. doi: 10.1214/23-AOS2276. URL <https://doi.org/10.1214/23-AOS2276>.
- Debashish Chakraborty, Eugene Yang, Daniel Khashabi, Dawn Lawrie, and Kevin Duh. Principled context engineering for RAG: Statistical guarantees via conformal prediction. In *Advances in Information Retrieval: 48th European Conference on Information Retrieval, ECIR 2026, Delft, The Netherlands, March 29–April 2, 2026, Proceedings, Part II*, pages 537–546, Berlin, Heidelberg, 2026. Springer-Verlag. ISBN 978-3-032-21299-3. doi: 10.1007/978-3-032-21300-6_45. URL https://doi.org/10.1007/978-3-032-21300-6_45.
- Prasanjit Dubey and Xiaoming Huo. Federated language models under bandwidth budgets: Distillation rates and conformal coverage, 2026. URL <https://arxiv.org/abs/2605.09986>.
- Etienne Gauthier, Francis Bach, and Michael I. Jordan. E-values expand the scope of conformal prediction, 2025. URL <https://arxiv.org/abs/2503.13050>.
- Isaac Gibbs and Emmanuel Candès. Adaptive conformal inference under distribution shift. In M. Ranzato, A. Beygelzimer, Y. Dauphin, P.S. Liang, and J. Wortman Vaughan, editors, *Advances in Neural Information Processing Systems*, volume 34, pages 1660–1672. Curran Associates, Inc., 2021. URL https://proceedings.neurips.cc/paper_files/paper/2021/file/0d441de75945e5acbc865406fc9a2559-Paper.pdf.
- Dan Hendrycks, Collin Burns, Steven Basart, Andy Zou, Mantas Mazeika, Dawn Song, and Jacob Steinhardt. Measuring massive multitask language understanding. In *International Conference on Learning Representations*, 2021. URL <https://openreview.net/forum?id=d7KBjmI3GmQ>.
- Steven R. Howard, Aaditya Ramdas, Jon McAuliffe, and Jasjeet Sekhon. Time-uniform Chernoff bounds via nonnegative supermartingales. *Probability Surveys*, 17:257 – 317, 2020. doi: 10.1214/18-PS321. URL <https://doi.org/10.1214/18-PS321>.
- Steven R. Howard, Aaditya Ramdas, Jon McAuliffe, and Jasjeet Sekhon. Time-uniform, nonparametric, nonasymptotic confidence sequences. *The Annals of Statistics*, 49(2):1055 – 1080, 2021. doi: 10.1214/20-AOS1991. URL <https://doi.org/10.1214/20-AOS1991>.

- Bror Hultberg, Dave Zachariah, and Antônio H. Ribeiro. Anytime-valid conformal risk control, 2026. URL <https://arxiv.org/abs/2602.04364>.
- Jens Lehmann, Robert Isele, Max Jakob, Anja Jentzsch, Dimitris Kontokostas, Pablo N. Mendes, Sebastian Hellmann, Mohamed Morsey, Patrick van Kleef, Sören Auer, and Christian Bizer. DBpedia – a large-scale, multilingual knowledge base extracted from Wikipedia. *Semantic Web*, 6(2):167–195, 2015. doi: 10.3233/SW-140134.
- Shuo Li, Sangdon Park, Insup Lee, and Osbert Bastani. TRAQ: Trustworthy retrieval augmented question answering via conformal prediction. In Kevin Duh, Helena Gomez, and Steven Bethard, editors, *Proceedings of the 2024 Conference of the North American Chapter of the Association for Computational Linguistics: Human Language Technologies (Volume 1: Long Papers)*, pages 3799–3821, Mexico City, Mexico, June 2024. Association for Computational Linguistics. doi: 10.18653/v1/2024.naacl-long.210. URL <https://aclanthology.org/2024.naacl-long.210/>.
- Charles Lu, Yaodong Yu, Sai Praneeth Karimireddy, Michael Jordan, and Ramesh Raskar. Federated conformal predictors for distributed uncertainty quantification. In Andreas Krause, Emma Brunskill, Kyunghyun Cho, Barbara Engelhardt, Sivan Sabato, and Jonathan Scarlett, editors, *Proceedings of the 40th International Conference on Machine Learning*, volume 202 of *Proceedings of Machine Learning Research*, pages 22942–22964. PMLR, 23–29 Jul 2023. URL <https://proceedings.mlr.press/v202/lu23i.html>.
- Vincent Plassier, Mehdi Makni, Aleksandr Rubashevskii, Eric Moulines, and Maxim Panov. Conformal prediction for federated uncertainty quantification under label shift. In Andreas Krause, Emma Brunskill, Kyunghyun Cho, Barbara Engelhardt, Sivan Sabato, and Jonathan Scarlett, editors, *Proceedings of the 40th International Conference on Machine Learning*, volume 202 of *Proceedings of Machine Learning Research*, pages 27907–27947. PMLR, 23–29 Jul 2023. URL <https://proceedings.mlr.press/v202/plassier23a.html>.
- Aaditya Ramdas, Peter Grünwald, Vladimir Vovk, and Glenn Shafer. Game-Theoretic Statistics and Safe Anytime-Valid Inference. *Statistical Science*, 38(4):576 – 601, 2023. doi: 10.1214/23-STS894. URL <https://doi.org/10.1214/23-STS894>.
- Jean Ville. *Étude critique de la notion de collectif*. Number 3 in Monographies des probabilités. Gauthier-Villars, Paris, 1939. URL <http://eudml.org/doc/192893>. Fascicule III.
- Vladimir Vovk, Ivan Petej, Ilia Nourtdinov, Ernst Ahlberg, Lars Carlsson, and Alex Gammerman. Retrain or not retrain: conformal test martingales for change-point detection. In Lars Carlsson, Zhiyuan Luo, Giovanni Cherubin, and Khuong An Nguyen, editors, *Proceedings of the Tenth Symposium on Conformal and Probabilistic Prediction and Applications*, volume 152 of *Proceedings of Machine Learning Research*, pages 191–210. PMLR, 08–10 Sep 2021. URL <https://proceedings.mlr.press/v152/vovk21b.html>.
- Ian Waudby-Smith and Aaditya Ramdas. Estimating means of bounded random variables by betting. *Journal of the Royal Statistical Society Series B: Statistical Methodology*, 86(1):1–27, 02 2024. ISSN 1369-7412. doi: 10.1093/jrsssb/qkad009. URL <https://doi.org/10.1093/jrsssb/qkad009>.

- Haifeng Wen, Osvaldo Simeone, and Hong Xing. Efficient federated conformal prediction with group-conditional guarantees, 2026. URL <https://arxiv.org/abs/2603.14198>.
- Rui Xu, Xingyuan Chen, Wenxing Huang, Minxuan Huang, Yun Xie, Weiyan Chen, and Sihong Xie. Federated conditional conformal prediction via generative models, 2025. URL <https://arxiv.org/abs/2510.13297>.
- Xiang Zhang, Junbo Zhao, and Yann LeCun. Character-level convolutional networks for text classification. In Corinna Cortes, Neil D. Lawrence, Daniel D. Lee, Masashi Sugiyama, and Roman Garnett, editors, *Advances in Neural Information Processing Systems*, volume 28, pages 649–657. Curran Associates, Inc., 2015. URL https://proceedings.neurips.cc/paper_files/paper/2015/hash/250cf8b51c773f3f8dc8b4be867a9a02-Abstract.html.

Supplementary Material

This supplement contains complete proofs of all six results stated in the main paper (Lemmas 4.5–4.6 and Theorems 4.7–4.12), with extended remarks on the cal-deviation budget, sticky vs. resetting alarms, and the tightness of the conditional-density clause placed after the corresponding proofs; and extended experimental results including the Lemma 4.5 sanity check, the Δ_{train} two-term form verification, real-world ablations (A2–A4), and necessity and robustness studies. We use the notation of the main paper throughout.

S1 Proofs

S1.1 Proof of Lemma 4.5 (one-step deployment null)

The proof proceeds in three steps. We first bound the conditional miscoverage relative to the population quantile (Step 1), then absorb the empirical-vs-population deviation on the cal-good event G_t (Step 2), then absorb retrieval-bandwidth quantization (Step 3). Throughout, the test pair (X_t, Y_t) is independent of \mathcal{F}_{t-1} by Assumption 4.2, and any quantity defined from past observations is \mathcal{F}_{t-1} -measurable.

Step 1 (population coverage). Recall the deployed-student score s_t^* from Section 2, and let q_t^{pop} denote the $(1 - \alpha)$ -quantile of $s_t^*(X, Y)$ under $(X, Y) \sim P^*$ (the score function is \mathcal{F}_{t-1} -measurable, so q_t^{pop} is too). Since $(X_t, Y_t) \mid \mathcal{F}_{t-1}$ has the same conditional law as the deployment-law marginal,

$$\mathbb{P}\left(s_t^*(X_t, Y_t) \leq q_t^{\text{pop}} \mid \mathcal{F}_{t-1}\right) \geq 1 - \alpha,$$

with equality under continuity. (The classical $1/(n_{\text{cal},t} + 1)$ split-conformal overshoot is a strictly weaker bound on the same quantity; we keep it inside b_t for compatibility with [Dubey and Huo, 2026] but the high-probability conditional analysis below does not need it.)

Step 2 (quantile reconstruction on G_t). On the event G_t , by the construction of G_t in (1),

$$|\hat{q}_t - q_t^{\text{pop}}| \leq c_q \sqrt{\log(2/\delta_t^{\text{cal}})/n_{\text{cal},t}} + \phi(B_t^{\text{cal}}).$$

By Assumption 4.3 the score CDF is $f_{\max,t}$ -Lipschitz in a neighborhood of q_t^{pop} [Dubey and Huo, 2026, Lemma 2], so on G_t ,

$$|\mathbb{P}(s_t^* \leq \hat{q}_t \mid \mathcal{F}_{t-1}) - \mathbb{P}(s_t^* \leq q_t^{\text{pop}} \mid \mathcal{F}_{t-1})| \leq \Delta_{\text{FL},t}.$$

Step 3 (score perturbation, variance-based). Under the dithered-quantization Assumption (B3) of [Dubey and Huo, 2026] the swarm score decomposes as $s_t^{\text{swarm}}(X_t, y) = s_t^*(X_t, y) + \bar{\xi}_t(X_t, y)$ with the dither average $\bar{\xi}_t = (1/K) \sum_i \xi_{i,t}$ satisfying $\mathbb{E}[\bar{\xi}_t \mid \mathcal{F}_{t-1}, X_t] = 0$ and, by independence of the per-node noise,

$$\mathbb{E}[\bar{\xi}_t^2 \mid \mathcal{F}_{t-1}, X_t] \leq V_{K,t} := \frac{1}{K^2} \sum_{i=1}^K v(B_{i,t}).$$

For any \mathcal{F}_{t-1} -measurable threshold u in the score-density neighborhood of Assumption 4.3, write $F_{|\bar{\xi}}^*(u) := F_{s_t^*|\bar{\xi}_t}(u | \mathcal{F}_{t-1}, X_t)$. Then

$$\mathbb{P}(s_t^{\text{swarm}} \leq u | \mathcal{F}_{t-1}, X_t) - \mathbb{P}(s_t^* \leq u | \mathcal{F}_{t-1}, X_t) = \mathbb{E}[F_{|\bar{\xi}}^*(u - \bar{\xi}_t) - F_{|\bar{\xi}}^*(u) | \mathcal{F}_{t-1}, X_t].$$

The strengthened conditional-density clause of Assumption 4.3 (the conditional density of s_t^* given $\bar{\xi}_t$ is bounded by $f_{\max,t}$ on the same neighborhood) makes $u \mapsto F_{|\bar{\xi}}^*(u)$ uniformly $f_{\max,t}$ -Lipschitz, so by Cauchy–Schwarz,

$$|\mathbb{P}(s_t^{\text{swarm}} \leq u | \mathcal{F}_{t-1}, X_t) - \mathbb{P}(s_t^* \leq u | \mathcal{F}_{t-1}, X_t)| \leq f_{\max,t} \mathbb{E}[|\bar{\xi}_t| | \mathcal{F}_{t-1}, X_t] \leq f_{\max,t} \sqrt{V_{K,t}}.$$

Taking expectation over $X_t | \mathcal{F}_{t-1}$ and recalling the definition of $\Delta_{\text{RAG},t}$,

$$|\mathbb{P}(s_t^{\text{swarm}}(X_t, Y_t) \leq u | \mathcal{F}_{t-1}) - \mathbb{P}(s_t^*(X_t, Y_t) \leq u | \mathcal{F}_{t-1})| \leq \Delta_{\text{RAG},t}.$$

Combine. On G_t , chaining Steps 1–3,

$$\begin{aligned} \mathbb{P}(s_t^{\text{swarm}}(X_t, Y_t) \leq \hat{q}_t | \mathcal{F}_{t-1}) &\geq \mathbb{P}(s_t^*(X_t, Y_t) \leq \hat{q}_t | \mathcal{F}_{t-1}) - \Delta_{\text{RAG},t} && \text{(Step 3)} \\ &\geq \mathbb{P}(s_t^*(X_t, Y_t) \leq q_t^{\text{pop}} | \mathcal{F}_{t-1}) - \Delta_{\text{RAG},t} - \Delta_{\text{FL},t} && \text{(Step 2)} \\ &\geq 1 - \alpha - \Delta_{\text{RAG},t} - \Delta_{\text{FL},t} && \text{(Step 1)} \\ &\geq 1 - \alpha - \Delta_{\text{RAG},t} - \Delta_{\text{FL},t} - \Delta_{\text{train},t} && (\Delta_{\text{train},t} \geq 0). \end{aligned}$$

Hence $\mathbb{E}[M_t | \mathcal{F}_{t-1}] \leq \alpha + \Delta_{\text{FL},t} + \Delta_{\text{RAG},t} + \Delta_{\text{train},t} \leq b_t$ on G_t . The $\Delta_{\text{train},t}$ slack in b_t absorbs training-side conservatism: it is bounded explicitly via the FTC chain of Section 2 (training-side distortion paragraph), inheriting the (B5') conditional-density clause of [Dubey and Huo, 2026, Corollary 3], and propagated across FPLD refresh events in Theorem 4.12. \square

Why the cal-deviation budget is not optional. Suppose one tried to skip the cal-deviation budget and instead use the marginal-over-calibration high-probability bound of [Dubey and Huo, 2026, Theorem 2] with a single fixed δ , centering the e-process at

$$b_t^{\text{marg}} := \alpha + \frac{1}{n_{\text{cal},t+1}} + f_{\max,t} \left(c_q \sqrt{\log(2/\delta)/n_{\text{cal},t}} + \phi(B_t^{\text{cal}}) \right) + \Delta_{\text{RAG},t} + \Delta_{\text{train},t}.$$

The marginal bound holds with probability $\geq 1 - \delta$ at any single t , but for sequential validity simultaneously over all t a union bound is needed and a fixed δ does not deliver one. On buffer realizations whose quantile deviation exceeds the centering at sufficiently many t , $\mathbb{E}[M_t | \mathcal{F}_{t-1}]$ exceeds b_t^{marg} pointwise and the supermartingale property fails; Ville's inequality cannot be applied. The summable budget $\{\delta_t^{\text{cal}}\}$ remedies this at the cost of an $O(\sqrt{\log t})$ inflation of $\Delta_{\text{FL},t}$.

S1.2 Proof of Lemma 4.6 (truncated supermartingale)

Nonnegativity. $Z_t \geq -b_t$, so $1 + \lambda_t Z_t \geq 1 - \lambda_t b_t \geq 0$ when $\lambda_t \leq 1/b_t$; inductively $E_t \geq 0$ and hence $\tilde{E}_t = E_t \mathbf{1}_{\Omega_{\text{cal},t}} \geq 0$.

Conditional mean. Since E_{t-1} , λ_t , and $\mathbf{1}_{\Omega_{\text{cal},t-1}}$ are \mathcal{F}_{t-1} -measurable, and $\mathbf{1}_{G_t}$ is \mathcal{F}_{t-1} -measurable by construction (Section 2), the indicator $\mathbf{1}_{\Omega_{\text{cal},t}} = \mathbf{1}_{\Omega_{\text{cal},t-1}} \mathbf{1}_{G_t}$ is \mathcal{F}_{t-1} -measurable. Hence

$$\begin{aligned} \mathbb{E}[\tilde{E}_t | \mathcal{F}_{t-1}] &= \mathbb{E}\left[E_{t-1} (1 + \lambda_t Z_t) \mathbf{1}_{\Omega_{\text{cal},t-1}} \mathbf{1}_{G_t} \mid \mathcal{F}_{t-1}\right] \\ &= E_{t-1} \mathbf{1}_{\Omega_{\text{cal},t-1}} \mathbf{1}_{G_t} (1 + \lambda_t \mathbb{E}[Z_t | \mathcal{F}_{t-1}]). \end{aligned}$$

On G_t , $\mathbb{E}[Z_t \mid \mathcal{F}_{t-1}] \leq 0$ by Lemma 4.5, so $\mathbf{1}_{G_t}(1 + \lambda_t \mathbb{E}[Z_t \mid \mathcal{F}_{t-1}]) \leq \mathbf{1}_{G_t} \leq 1$. Therefore

$$\mathbb{E}[\tilde{E}_t \mid \mathcal{F}_{t-1}] \leq E_{t-1} \mathbf{1}_{\Omega_{\text{cal},t-1}} = \tilde{E}_{t-1}. \quad \square$$

S1.3 Proof of Theorem 4.7 (alarm validity)

(\tilde{E}_t) is a nonnegative supermartingale with $\mathbb{E}\tilde{E}_0 = 1$ by Lemma 4.6, so Ville's inequality [Ville, 1939, Howard et al., 2020] gives $\mathbb{P}(\sup_t \tilde{E}_t \geq 1/\delta_e) \leq \delta_e$. On Ω_{cal} , $\tilde{E}_t = E_t$ for all t . Splitting on Ω_{cal} ,

$$\mathbb{P}\left(\sup_t E_t \geq 1/\delta_e\right) \leq \mathbb{P}\left(\sup_t \tilde{E}_t \geq 1/\delta_e\right) + \mathbb{P}(\Omega_{\text{cal}}^c) \leq \delta_e + \delta_{\text{cal}}. \quad \square$$

S1.4 Proof of Theorem 4.9 (Hoeffding envelope)

$Z_s \in [-b_s, 1 - b_s]$ has range 1, so by Hoeffding's lemma applied conditionally on \mathcal{F}_{s-1} ,

$$\mathbb{E}[\exp(\lambda Z_s) \mid \mathcal{F}_{s-1}] \leq \exp\left(\lambda \mathbb{E}[Z_s \mid \mathcal{F}_{s-1}] + \frac{\lambda^2}{8}\right).$$

By Lemma 4.5, on G_s we have $\mathbb{E}[Z_s \mid \mathcal{F}_{s-1}] \leq 0$, so $\mathbf{1}_{G_s} \mathbb{E}[\exp(\lambda Z_s) \mid \mathcal{F}_{s-1}] \leq \mathbf{1}_{G_s} \exp(\lambda^2/8)$. For each fixed $\lambda \geq 0$ the truncated exponential process

$$\tilde{W}_t^\lambda := \exp(\lambda S_t - \lambda^2 t/8) \mathbf{1}_{\Omega_{\text{cal},t}}$$

is therefore a nonnegative supermartingale with $\mathbb{E}\tilde{W}_0^\lambda = 1$ (the same indicator-truncation argument as Lemma 4.6). Ville's inequality gives $\mathbb{P}(\exists t : \tilde{W}_t^\lambda \geq 1/\delta_\lambda) \leq \delta_\lambda$, equivalently $\mathbb{P}(\exists t : S_t \geq \lambda^{-1} \log(1/\delta_\lambda) + \lambda t/8 \text{ on } \Omega_{\text{cal},t}) \leq \delta_\lambda$. Stitching over a discrete grid $\lambda_k = 2^{-k}$ ($k = 0, 1, 2, \dots$) with budgets $\delta_k = \delta_e c_\zeta / (k+1)^2$ ($c_\zeta = 6/\pi^2$) by the union-bound argument of [Howard et al., 2021] produces the displayed boundary on the event Ω_{cal} ; the constant $c_H \leq 1.7$ is from their Eq. (14). Splitting on Ω_{cal} then yields $\mathbb{P}(\exists t : S_t > u_t(\delta_e)) \leq \delta_e + \delta_{\text{cal}}$. The stopping-time corollary follows by evaluating at $t = \tau$ inside the joint high-probability event. \square

S1.5 Proof of Theorem 4.11 (safe adaptive control)

The post-action quantities $(\hat{q}_t, B_{\bullet,t}, \hat{P}_t)$ at time t are \mathcal{F}_{t-1} -measurable by hypothesis. Hence $b_t = \alpha + 1/(n_{\text{cal},t} + 1) + \Delta_{\text{FL},t} + \Delta_{\text{RAG},t} + \Delta_{\text{train},t}$ and the calibration-good event G_t both remain \mathcal{F}_{t-1} -measurable, with the same per-step bound $\mathbb{P}(G_t) \geq 1 - \delta_t^{\text{cal}}$ applying since δ_t^{cal} is fixed by the predictable budget schedule. The conclusion of Lemma 4.5 applies as written. The supermartingale calculation in Lemma 4.6 proceeds without modification, as does the truncated Hoeffding bound underlying Theorem 4.9. Validity is therefore preserved under the entire intervention path. \square

Sticky vs. resetting alarms. Algorithm 1 does not reset E_t after an alarm. The sticky version preserves $\mathbb{P}(\sup_t E_t \geq 1/\delta_e) \leq \delta_e + \delta_{\text{cal}}$ over the entire trajectory but does not give post-intervention re-tests. A reset variant divides δ_e into per-epoch budgets $\delta_{e,k}$ with $\sum_k \delta_{e,k} \leq \delta_e$ and starts a fresh e-process at each reset; Theorem 4.7 applies to each epoch independently and a union bound recovers the global guarantee. Both variants are safe; we default to sticky.

S1.6 Proof of Theorem 4.12 (training propagation)

Theorem 1 of [Dubey and Huo, 2026] gives, for each training event r , $\bar{K}^{(r)} := \mathbb{E}_{X \sim P_X^*}[\text{KL}(P^*(\cdot|X) \parallel \hat{P}^{(r)}(\cdot|X))] \leq \mathcal{R}_r$ with probability $\geq 1 - \delta_r$. The chain of the training-side distortion paragraph in Section 2 ((B5') of Assumption 4.3 + indicator-difference + FTC + the splitting $\mathbb{E}_{P^*}|\Delta_t| \leq \bar{K}_t + \sqrt{2\bar{K}_t}$ via $\log(1+t) \leq t$ and Pinsker; [Dubey and Huo, 2026, Corollary 3]) gives, on each training-good event with $\bar{K}_t := \bar{K}^{(r(t))}$,

$$\Delta_{\text{train},t} \leq f_{\max,t} \mathbb{E}_{X,Y}|\Delta_t(X,Y)| \leq f_{\max,t}(\bar{K}_t + \sqrt{2\bar{K}_t}) \leq f_{\max,t}(\mathcal{R}_{r(t)} + \sqrt{2\mathcal{R}_{r(t)}}).$$

Union bound over training events with $\sum_r \delta_r \leq \delta_{\text{train}}$ yields the simultaneous-in- t statement on an event of probability $\geq 1 - \delta_{\text{train}}$. \square

Tightness and the conditional-density clause. The two-term form $\Delta_{\text{train},t} = f_{\max,t}(\mathcal{R}_{r(t)} + \sqrt{2\mathcal{R}_{r(t)}})$ follows [Dubey and Huo, 2026, Corollary 3] under the clause (B5') of Assumption 4.3. In the small- \mathcal{R} regime the second summand dominates, recovering the Pinsker- $\sqrt{\cdot}$ shape; the linear summand is the price paid for matching base FC-RAG's exact form. Absent the clause (B5'), the FTC step fails and only the weaker $O(f_{\max,t} \mathcal{R}^{1/4})$ rate is recoverable via Markov truncation. Both the alarm validity and the cumulative envelope are insensitive to this choice; only the absolute scale of b_t shifts.

S2 Extended experimental results

S2.1 E10: conditional bound on the cal-good event

We sample 1000 buffer realizations of size $n_{\text{cal}} = 100$, scores Uniform[0, 1], $\alpha = 0.10$, $\delta_{\text{cal}} = 0.05$, $f_{\max} = 1.0$. For each buffer we compute the empirical $(1 - \alpha)$ -quantile \hat{q} , the cal-good bound b_t at $t \in \{1, 10, 10^2, 10^3, 10^4\}$ (with $\delta_t^{\text{cal}} = 6\delta_{\text{cal}}/(\pi^2 t^2)$), and check whether the conditional miscoverage rate $\mathbb{P}(s > \hat{q} \mid \hat{q})$ exceeds b_t . The violation rate is 0.0000 across all 5000 buffer/horizon pairs, confirming Lemma 4.5 pointwise. The bound widens with t as expected ($b_1 = 0.280$, $b_{10^4} = 0.471$, via the $\sqrt{\log(2/\delta_t^{\text{cal}})}$ inflation in $\Delta_{\text{FL},t}$), while the realized conditional miscoverage stays at $\alpha = 0.10$ regardless of t . The horizon-dependent inflation is the price of the conditional (vs. marginal) form; E8 quantifies it as a $1.07\times$ – $2.72\times$ factor over the cost-relevant range.

S2.2 E5: Δ_{train} two-term form verification

For Bernoulli pairs (p, q) on a 5×5 grid with FPLD-distillation residuals drawn from Beta(2, 2), the empirical ratio of $|p - q|$ to $f_{\max}(\mathcal{R} + \sqrt{2\mathcal{R}})$ stays below 1 in 100% of 20 sampled pairs (max ratio 0.91, mean ratio 0.65). The two-term form from [Dubey and Huo, 2026, Corollary 3] holds tightly under the clause (B5'): this is a numerical witness for Theorem 4.12.

S2.3 Real-world ablations: A2, A3, A4 in detail

Drift types (A2). On DBpedia (the genuine-drift benchmark), alarm rates rank by drift severity as expected: `no_drift` 0.00, `sudden` 1.00, `gradual` 0.67, `periodic` 0.33.

Sudden onset gives the strongest signal; gradual interpolation slows evidence accumulation; periodic schedules return to cal subjects every period and dilute the signal. On MMLU (in-cal) and AG News (priors-recoverable), all schedules including sudden stay near zero alarm, mirroring A1’s discriminative behavior.

Heterogeneous bandwidth (A3). On MMLU across four bandwidth configurations, alarm rate is monotone in average bandwidth: `uniform_high` ($B_i = 10$, alarm 0.27); `mixed_one_weak` ($B_i = (3, 10, 10, 10)$, alarm 0.00); `mixed_two_weak` ($B_i = (3, 3, 10, 10)$, alarm 0.00); `uniform_low` ($B_i = 4$, alarm 0.00). Higher bandwidth shrinks Δ_{RAG} , tightens b_t , and lifts detection power, exactly the dependence the slack decomposition predicts (Theorem 4.7).

Multi-refresh (A4). On MMLU with two FPLD-style refresh events (perturbation noise schedule $0.5 \rightarrow 0.25 \rightarrow 0$ with transitions at $t \in \{500, 1500\}$), b_t shrinks at each refresh as the training residual $\mathcal{R}_{r(t)}$ drops, and the e-process growth rate recalibrates accordingly, the predicted behavior under Theorem 4.12. Final miscoverage is 0.120 ± 0.027 across 15 trajectories.

S2.4 Necessity and robustness of the construction

Two construction choices in §3 are not optional. The cal-deviation budget $\{\delta_t^{\text{cal}}\}$ is needed because adversarial buffer realizations make a marginal-bound centering b_t^{marg} fail the supermartingale property; on uniform-Bernoulli null streams both our construction and the marginal variant alarm at 0.0000 (the inflation only kicks in on the exponentially-decaying tail event the budget is designed to control), so the budget functions as a theoretical safety net rather than an empirical-power booster. Predictability is needed at the controller layer: a non-predictable controller that switches bandwidth based on M_t rather than \mathcal{F}_{t-1} -measurable evidence inflates Type-I from 0.0070 (predictable, within δ_e) to 0.1010 (non-predictable, above $\delta_e + \delta_{\text{cal}} = 0.10$), a $14.4\times$ violation of Theorem 4.7 confirming the predictability assumption of Theorem 4.11 is empirically load-bearing.

The bettor and hyperparameters are robust. Against three constant- λ baselines ($\lambda \in \{0.32, 1.61, \bar{\lambda} = 3.23\}$, the slack-admissibility cap), the predictable-plug-in aGRAPA bettor matches all three under the null and on large drift but dominates by $4.9\times$ on small drift (0.348 alarm rate vs. best constant- λ ’s 0.071, Figure 7); aGRAPA is the only choice that is uniformly competitive across drift sizes. One-at-a-time sweeps over $\alpha \in \{0.05, 0.10, 0.15, 0.20\}$, $\delta_e \in \{0.01, 0.025, 0.05, 0.10\}$, and the λ -cap factor $\in \{0.25, 0.5, 0.75, 1.0\}$ (12 configurations in total) leave Type-I within the corresponding δ_e in every configuration and detection power ≥ 0.81 throughout (Figure 8), so the canonical choices used elsewhere in the paper are not load-bearing in their specific values.

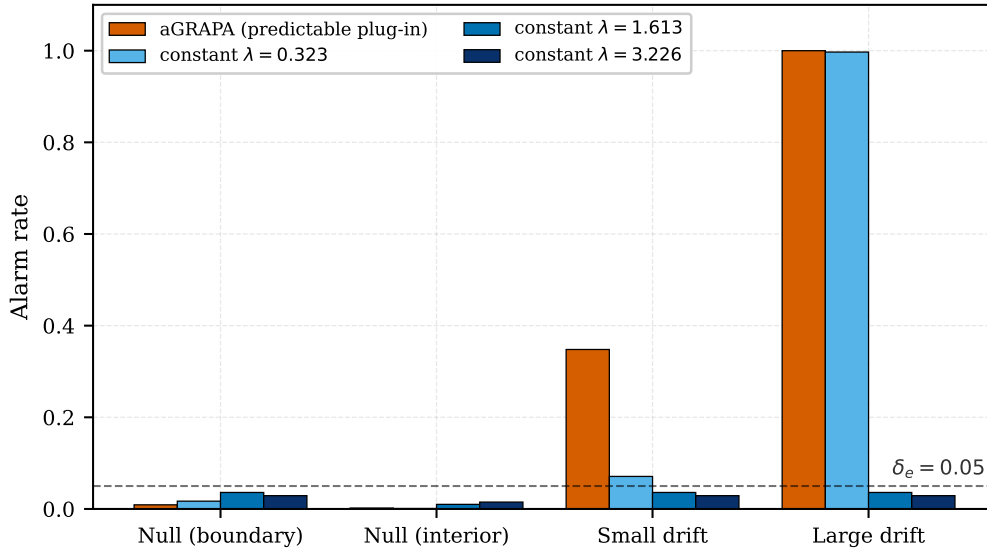


Figure 7: Alarm rate of aGRAPA vs. three constant- λ baselines across four regimes (two null, two drift). Constant- λ matches aGRAPA on large drift but undercovers small drift by 4.9 \times ; aGRAPA is the only better that is uniformly competitive.

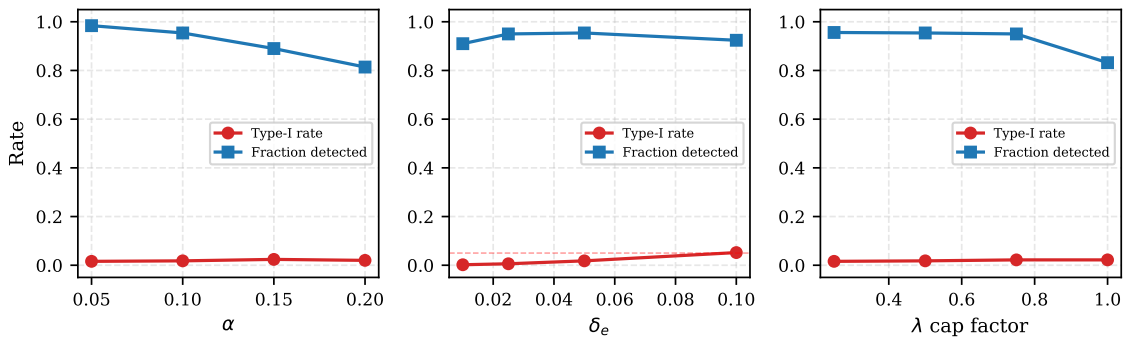


Figure 8: Type-I (red) and detection power (blue) under one-at-a-time sweeps over α , δ_e , and the λ -cap factor. Type-I tracks δ_e in every configuration; power stays ≥ 0.81 throughout.